QIRT10 http://dx.doi.org/10.21611/qirt.2010.147
10th International Conference on Quantitative InfraRed Thermography
July 27-30, 2010, Québec (Canada)

On-off modulated thermography of composite material and signal processing

Guo Xingwang*, Li Zheng*, Liu Yingtao**
* School of Mechanical Engineering and Automation, Beihang University, Beijing 100191, P. R. China, xingwangguo@buaa.edu.cn
** Beijing Institute of Aeronautical Materials, Beijing 100095, P. R. China

Abatract

To extract the phase information from the waved signal in on-off MT, the discrete Fourier series (DFS) correlation coefficient and cosine distance method were proposed and compared with traditional ones. A glass fiber reinforced plastic (GFRP) specimen with artificial embedded defects was detected by on-off MT. The image sequences were processed with 4-point method, DFT, S method, correlation coefficient method and cosine distance method respectively, and several ways of selecting reference signal were discussed. The results were quantitatively compared by SNR and shows that, the proposed three methods are effective in on-off MT as well as in sinusoidal MT.

Keywords: modulated thermography, on-off modulation, signal processing, composite material

1. Introduction

Composite materials are widely used in aerospace structure thanks to their high specific strength, high specific rigidity, vibration resistance and corrosion resistance. To satisfy the increasing safety level, nondestructive testing (NDT) of composite materials is necessary. In the last two decade, with the development of infrared and signal processing technology and the effort of many research groups, infrared thermography became an attractive NDT technique, and was considered as an useful tool for NDT&E of aerospace materials[1-3]. There are several active thermographic techniques[3], such as pulsed thermography (PT)[4], modulated thermography (MT) known as lock-in thermography (LT)[5-6], vibrothemography (VT) [7]and so on. By comparison to PT, MT requires lower heat energy, is less sensitive to non-uniform heating and non-uniform skin emissivity, and has better adaptability to curved surface, but requires longer testing time. MT occupies an important position in IR NDT, and has been successfully used in inspection of aerospace materials[2-6], concrete[8] and some other materials The classic signal processing technique for MT is the well known four-point method which is deduced from sinusoidal signal. A big error will occur in the phase information obtained by the four-point method when the signal processed is not sinusoidal signal. As a facility tool of frequency domain analysis, Fourier transform has good effect in PT [4,9] as well as in MT.

In this paper, on-off modulated thermography of composite materials and its image sequence processing are studied. The classic signal process methods are reviewed. In order to extract the phase information of the non-sinusoidal signal in on-off MT, discrete Fourier series (DFS) method, correlation coefficient method and cosine distance method are proposed and demonstrated. The processing results were quantitatively compared by the SNR of defects

2. Signal processing methods of MT

2.1. Four-point method

The most frequently used method to process MT signal is four-point method which retrieves the phase ϕ and magnitude A from four equidistant signal data points S_1、S_2、S_3 and S_4 recorded during one cycle of the modulation:

$$\phi = \arctan\left(\frac{S_3 - S_1}{S_4 - S_2}\right) \quad (1)$$

$$A = \sqrt{(S_3 - S_1)^2 + (S_4 - S_2)^2} \quad (2)$$

The basic four-point method is exact only for sinusoidal waveform and is affected by noise. The noise can be decreased in part by averaging of several data points in one cycle or multiple cycles.

2.2. Discrete Fourier series method

If the signal $x(t)$ ($0 \le t < T$, T is the width of the truncation time window) is extended to a periodic signal whose period is T (angular frequency $\omega_0 = 2\pi / T$), then $x(t)$ ($0 \le t < T$) can be described in frequency domain by Fourier series (FS) expansion:

$$x(t) = a_0 + \sum_{k=1}^{\infty} (a_k \cos k\omega_0 t + b_m \sin k\omega_0 t) = A_0 + \sum_{k=1}^{\infty} A_k \cos(k\omega_0 t + \varphi_k) \quad (3)$$

with

$$a_0 = A_0 = \frac{1}{T}\int_0^T x(t)dt \quad (4)$$

$$a_k = \frac{2}{T}\int_0^T x(t)\cos k\omega_0 t dt \quad (5)$$

$$b_k = \frac{2}{T}\int_0^T x(t)\sin k\omega_0 t dt \quad (6)$$

$$A_k = \sqrt{a_k^2 + b_k^2} \quad (7)$$

$$\varphi_k = \arctan\frac{-b_k}{a_k} \quad (8)$$

where A_0 is the DC part, $k = 1, 2, 3\text{L}$.

Suppose N equidistant data points are sampled in each period T, then the sampling interval is $T_s = T / N$, the data points are at time $t = nT / N$ ($n = 0, 1, 2, \text{L}\ , N-1$). Let $x(n)$ express the discrete form of $x(t)$ after sampling, then the discrete form of Eq.(3), i.e. the discrete Fourier series (DFS) is given by:

$$x(n) = A_0 + \sum_{k=1}^{\infty}(a_k \cos\frac{2k\pi n}{N} + b_k \sin\frac{2k\pi n}{N}) = A_0 + \sum_{k=1}^{\infty} A_k \cos(\frac{2k\pi n}{N} + \varphi_k) \quad (9)$$

With

$$a_0 = A_0 = \frac{1}{N}\sum_{n=0}^{N-1} x(n) \quad (10)$$

$$a_k = \frac{2}{N}\sum_{n=0}^{N-1} x(n)\cos\frac{2k\pi n}{N} \quad (11)$$

$$b_k = \frac{2}{N}\sum_{n=0}^{N-1} x(n)\sin\frac{2k\pi n}{N} \quad (12)$$

$$A_k = \sqrt{a_k{}^2 + b_k{}^2} \quad (13)$$

$$\varphi_k = \arctan(\frac{-b_k}{a_k}) \quad (14)$$

When T takes k times of the modulation period in MT, the amplitude and phase at the modulation frequency is given by A_k and φ_k respectively.

2. 3. Discrete Fourier transform method

If the signal $x(t)$ ($0 \le t < T$, T is the width of the truncation time window) is sampled with sampling interval $T_s = T / N$, then the discrete signal $x(n)$ $(n = 0, 1, 2, \text{L}\ N-1)$ is obtained and can be analyzed in frequency domain with discrete Fourier transform (DFT).

The DFT is expressed as

$$X(k) = \frac{1}{N}\sum_{n=1}^{N-1} x(n)e^{-j\frac{2\pi kn}{N}} \quad (k = 0, 1, 2\text{L}\ , N-1) \quad (15)$$

The inverse DFT (IDFT) is expressed as

$$x(n) = \sum_{k=0}^{N-1} X(k)e^{j\frac{2\pi kn}{N}} \quad (n = 0, 1, 2\text{L}\ , N-1) \quad (16)$$

where N is the number of the discrete data points, n the serial number of the discrete data in time domain, $x(n)$ the signal value at the time $t = nT_s$, k the serial number of the discrete data in frequency domain,

$X(k)$ the data value at the frequency $f = kf_0$, f_0 the frequency resolution.

When T takes k times of the modulation period in MT, the amplitude and phase at the modulation frequency can be derived from $X(k)$, i.e. $A_k = |X(k)|$, $\varphi_k = \angle X(k)$.

Another form of Eq.(15) is

$$X(k) = \frac{1}{N}\sum_{n=0}^{N-1} x(n)\cos(\frac{2\pi kn}{N}) - j\frac{1}{N}\sum_{n=0}^{N-1} x(n)\sin(\frac{2\pi kn}{N}) = a_k - jb_k \qquad (17)$$

with

$$a_k = \frac{1}{N}\sum_{n=0}^{N-1} x(n)\cos(\frac{2\pi kn}{N}) \qquad (18)$$

$$b_k = \frac{1}{N}\sum_{n=0}^{N-1} x(n)\sin(\frac{2\pi kn}{N}) \qquad (19)$$

The amplitude and phase corresponding to $X(k)$ is

$$A_k = \sqrt{a_k{}^2 + b_k{}^2} \qquad (20)$$

$$\varphi_k = \arctan(\frac{-b_k}{a_k}) \qquad (21)$$

By comparing Eqs. (18)~(21) with Eqs. (11)~(14), it can be known that, the amplitude solved by DFT is half of that by DFS, and the phase is the same. This is due to fact that DFT describes the signal in two side frequency domain, but FDS does in single side.

2.4. Correlation method

Since the cross correlation function of two periodic signals is still a periodic signal with the same period and the phase information can be kept, it can be applied to retrieve the phase-shift of the two signals. Due to fact that the noise and the reference signal are not correlated, the correlation method can extract the effective information from a signal disturbed by noise.

Assume the signal $x(t)$ is a periodic signal whose period is T, then it can be expressed by Fourier series as Eq. (3). Select $y_1(t) = \cos\omega t$ and $y_2(t) = \sin\omega t$ as two reference signals, when $T_1 \to \infty$ or T_1 equals an integer times of T, consider the orthogonality of harmonic functions, the cross correlation functions of $x(t)$ with $y_1(t)$ and $y_2(t)$ are

$$R_{xy1}(0) = \lim_{T_1\to\infty}\frac{1}{T_1}\int_{.0}^{T_1} x(t)y_1(t)dt = \frac{A_1}{2}\cos\varphi_1 \qquad (22)$$

and

$$R_{xy2}(0) = \lim_{T_1\to\infty}\frac{1}{T_1}\int_{.0}^{T_1} x(t)y_2(t)dt = -\frac{A_1}{2}\sin\varphi_1 \qquad (23)$$

respectively. The phase and amplitude at the angular frequency ω is given by

$$\varphi_1 = \arctan\frac{-R_{xy2}(0)}{R_{xy1}(0)} \qquad (24)$$

$$A_1 = 2\sqrt{R_{xy1}^2(0) + R_{xy12}^2(0)} \qquad (25)$$

Let $x(n)$, $y_1(n)$ and $y_2(n)$ express the discrete form of $x(t)$, $y_1(t)$ and $y_2(t)$ after sampling respectively. If there are N sampling points in one period T (i.e the sampling interval is $T_s = T/N$), when $N_1 \to \infty$ or N_1 is an integrer times of N, the discretization forms of Eqs. (22) and (23) can be expressed as

$$R_{xy1}(0) = \frac{1}{N_1}\sum_{n=0}^{N_1-1} x(n)y_1(n) \qquad (26)$$

and

$$R_{xy2}(0)=\frac{1}{N_1}\sum_{n=0}^{N_1-1}x(n)y_2(n) \qquad (27)$$

respectively.

The phase and amplitude at the angular frequency ω then can be obtained by substituting Eqs. (26) and (27) into Eqs. (24) and (25).

By comparing Eqs. (24)~(27) with Eqs. (11)~(14), it can be seen that φ_1 and A_1 derived by correlation method has no difference with $\varphi_{k=1}$ and $A_{k=1}$ derived by DFS in trigonometric function form.

Although DFS, DFT and correlation method are three different analysis means, there is no essential difference in their computation processes and results, and the obtained phase is the same, therefore, their phase extraction abilities are equivalent.

2.5. Correlation coefficient method and included angle cosine method

Consider the thermal signal with N_1 sampling points as a N_1-dimension vector, then the signal can be analyzed by the methods to describe the similarity of two vectors. Here correlation coefficient (CC) method and included angle cosine (IAC) method are presented.

Assume the discrete form of the temperature signal $x(t)$ and $y(t)$ are $x(n)$ and $y(n)$ respectively, where n designates the time increment, then the correlation coefficient is expressed as:

$$\rho_{xy}=\frac{\sum_{n=0}^{N_1-1}[x(n)-\mu_x][y(n)-\mu_y]}{\sqrt{\sum_{n=0}^{N_1-1}[x(n)-\mu_x]^2\cdot\sum_{n=0}^{N_1-1}[y(n)-\mu_y]^2}},\quad (-1\le\rho_{xy}\le 1) \qquad (28)$$

where μ_x and μ_y are the DC parts of $x(t)$ and $y(t)$ respectively.

The included angle cosine is expressed as:

$$Q_{xy}=\frac{\sum_{n=0}^{N_1-1}x(n)y(n)}{\sqrt{\sum_{n=0}^{N_1-1}x^2(n)\sum_{n=0}^{N_1-1}y^2(n)}},\quad (-1\le Q_{xy}\le 1) \qquad (29)$$

By comparing Eq. (28) with Eq. (29), it can be seen that the difference between the correlation coefficient and the included angle cosine is whether the DC component is subtracted before.

The correlation coefficient is actually the correlation coefficient function at zero time, and its continuous form is expressed as:

$$\rho_{xy}(0)=\frac{\lim_{T_1\to\infty}\frac{1}{T_1}\int_0^{T_1}[x(t)-\mu_x)]\left[y(t)-\mu_y\right]dt}{\sqrt{\lim_{T_1\to\infty}\frac{1}{T_1}\int_0^{T_1}\left[x(t)-\mu_x\right]^2dt\cdot\lim_{T_1\to\infty}\frac{1}{T_1}\int_0^{T_1}\left[y(t)-\mu_y\right]^2dt}}=\frac{R_{xy}(0)-\mu_x\mu_y}{\sigma_x\sigma_y},\quad (-1\le\rho_{xy}(0)\le 1) \qquad (30)$$

where $R_{xy}(0)$ is the correlation function at 0 time, σ_x and σ_y the standard deviation of $x(t)$ and $y(t)$ respectively.

In a similar way, the continuous form of the included angle cosine is expressed as:

$$Q_{xy}=\frac{\lim_{T_1\to\infty}\frac{1}{T_1}\int_0^{T_1}x(t)y(t)dt}{\sqrt{\lim_{T_1\to\infty}\frac{1}{T_1}\int_0^{T_1}x^2(t)dt\cdot\lim_{T_1\to\infty}\frac{1}{T_1}\int_0^{T_1}y^2(t)dt}}=\frac{R_{xy}(0)}{x_{rms}y_{rms}},\quad (-1\le Q_{xy}\le 1) \qquad (31)$$

where x_{rms} and y_{rms} are the root mean square values of $x(t)$ and $y(t)$ respectively.

If μ_x=0 and μ_y=0, then

http://dx.doi.org/10.21611/qirt.2010.147

$$\rho_{xy}(0) = Q_{xy} \qquad (32)$$

If $x(t)$ is a general periodic signal expressed as Eq. (3), and $y(t)$ is selected as

$$y(t) = \mu_y + B_1 \cos(\omega t + \phi_1) \qquad (33)$$

we have

$$R_{xy}(0) = \mu_x \mu_y + \frac{A_1 B_1}{2} \cos(\varphi_1 - \phi_1) \qquad (34)$$

Substitute Eq. (34) into Eq.(30), we have

$$\rho_{xy}(0) = \frac{A_1}{\sqrt{2} \cdot \sigma_x} \cos(\varphi_1 - \phi_1) \qquad (-1 \le \rho_{xy}(0) \le 1) \qquad (35)$$

So the correlation coefficient has a proportional relation with $\cos(\varphi_1 - \phi_1)$.

Substitute Eq. (34) into Eq. (31), we have

$$Q_{xy} = \frac{A_1}{\sqrt{2} \cdot x_{rms}} \cos(\varphi_1 - \phi_1) + \frac{\sqrt{2} \cdot \mu_x \mu_y}{B_1 x_{rms}} \quad (-1 \le Q_{xy} \le 1) \qquad (36)$$

So the included angle cosine has a linear relation with $\cos(\varphi_1 - \phi_1)$. Specially, if μ_y=0, the included angle cosine has a proportional relation with $\cos(\varphi_1 - \phi_1)$.

Similarly, if $y(t)$ is selected as

$$y(t) = \mu_y + B_1 \sin(\omega t + \phi_1) = \mu_y + B_1 \cos(\omega t + \phi_1 - \pi/2) \qquad (37)$$

we have

$$\rho_{xy}(0) = \frac{A_1}{\sqrt{2} \cdot \sigma_x} \cos(\varphi_1 - \phi_1 + \pi/2) \qquad (-1 \le \rho_{xy}(0) \le 1) \qquad (38)$$

$$Q_{xy} = \frac{A_1}{\sqrt{2} \cdot x_{rms}} \cos(\varphi_1 - \phi_1 + \pi/2) + \frac{\sqrt{2} \cdot \mu_x \mu_y}{B_1 x_{rms}} \quad (-1 \le Q_{xy} \le 1) \qquad (39)$$

Both correlation coefficient method and included angle cosine method need a reference signal. Let $x_i(n)$ be the signal corresponding to the pixel i in thermal image sequence, and $y(n)$ be the reference signal, one can calculate the arc cosine of the correlation coefficient and/or the arc cosine of the included angle cosine between $x_i(n)$ and $y(n)$, and draw an image according to the phase values although the arc cosine values are not the real phase ($\varphi_1 - \phi_1$) or ($\varphi_1 - \phi_1 + \pi/2$). The reference signal $y(n)$ has several choice: the data in defect area, sound area, and mixed area, the mean value of all pixels, a sinusoidal (or cosine) signal with the modulation frequency.

3. Experiment and data processing

3.1. Experimental setup

The schematic illustration of the experimental setup is shown in Fig. 1. The specimen was periodically heating by halogen lamps (total 1.1kW) controlled by an on-off controller at a modulation frequency. The surface temperature field was recorded by an infrared camera with 320×240 pixel configuration. The computer and application program were used to integrate the whole system and implement the image sequence processing.

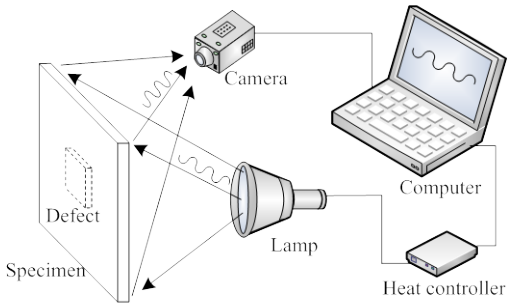

Fig.1. *Schematic experimental setup of MT*

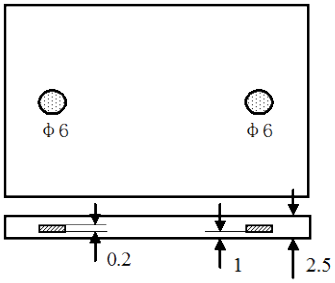

Fig. 2. *the sketch of GFRP specimen*

The specimen was a GFRP panel of 2.5 mm thickness containing 2 artificial Teflon® inserts of 6 mm diameter at 1 mm depth, as shown in Fig. 2. Every insert consists of two 0.1 mm-thick Teflon layers.

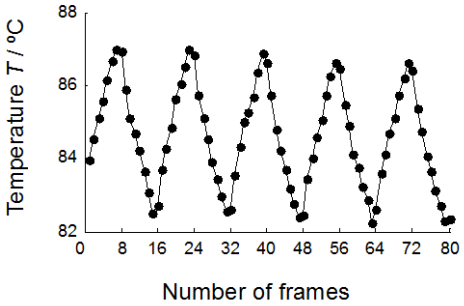

Fig.3. *Surface temperature evolution*

3.2. Data processing

The modulation period was set to 32s, the sampling interval was set to 2s, and 5 cycles data was recorded in the stationary regime, so 80 images was acquired by the infrared camera. The surface temperature evolution at one of the pixels is shown in Fig. 3. A typical raw image is shown in Fig. 4(a). No defect information can be seen in the raw image because of uneven heating and noise.

The phase images obtained by the average 4-point method, DFS method, correlation coefficient (CC) method and included angle cosine (IAC) method and are shown as Fig.4(b)~(o) respectively. The reference signal for the last two method was selected as the data in defect area, sound area, and mixed area, the mean value of all pixels, a sinusoidal and cosine signal with the modulation frequency respectively, as indicated in the figures.

(a) Raw image

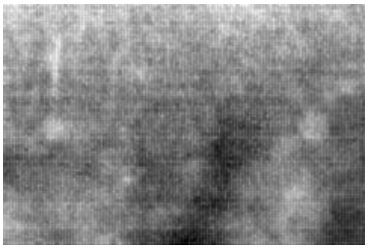

(b) average 4-point, SNR=0.71

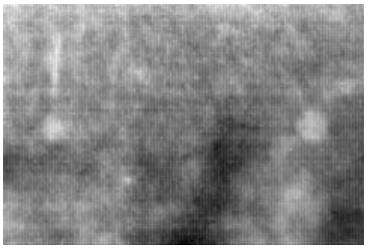

(c) DFS, SNR=1.30

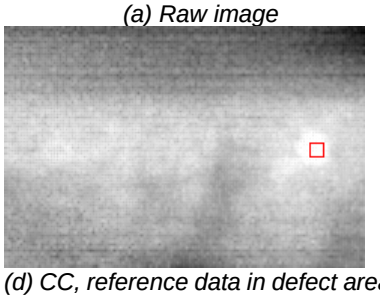

(d) CC, reference data in defect area, SNR=1.85, (inversed)

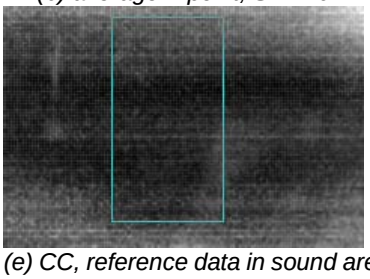

(e) CC, reference data in sound area, SNR=0.19

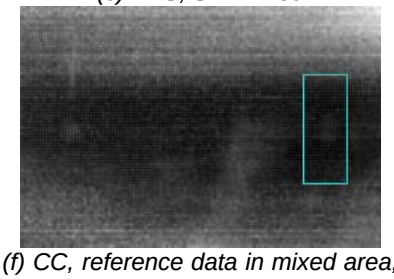

(f) CC, reference data in mixed area, SNR=0.94

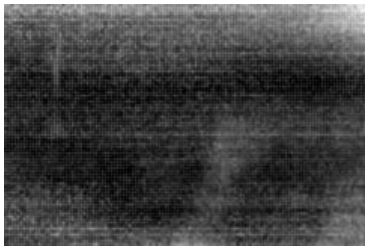

(g) CC, reference data takes mean value of all pixels, SNR=0.22

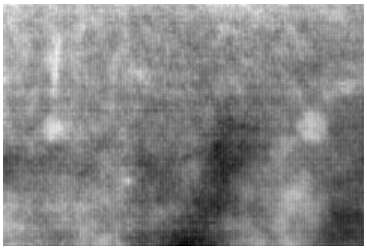

(h) CC, sinusoidal reference signal, SNR=1.37, (inversed)

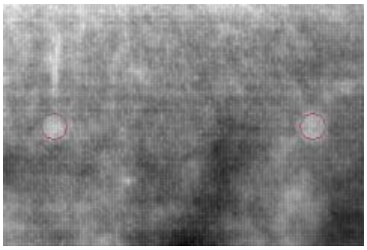

(i) CC, cosine reference signal, SNR=1.21, (inversed)

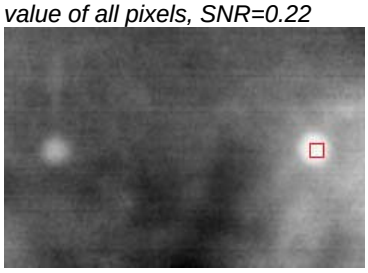

(j) IAC, reference data in defect area, SNR=3.10, (inversed)

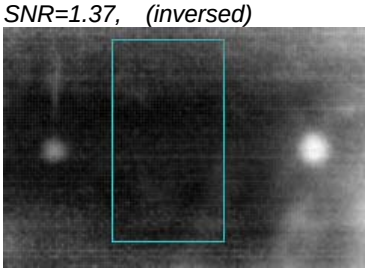

(k) IAC, reference data in sound area, SNR=2.38

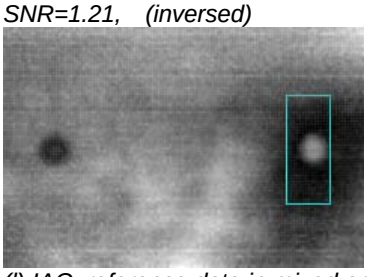

(l) IAC, reference data in mixed area, SNR=1.14

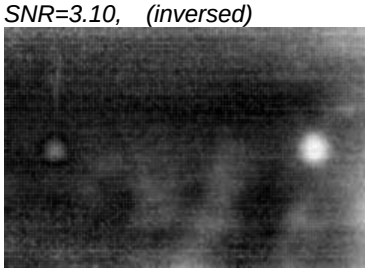

(m) IAC, reference data takes mean value of all pixels, SNR=2.49

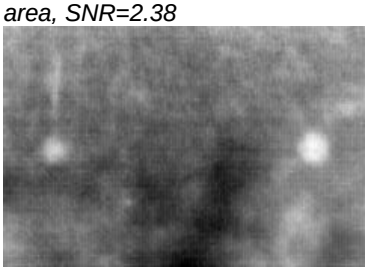

(n) IAC, sinusoidal reference signal, SNR=2.76 (inversed)

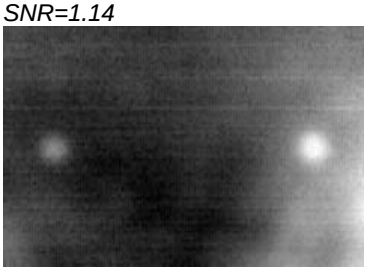

(o) IAC, cosine reference signal, SNR=2.14

Fig.4. *The resulting phase images of various methods (except (a))*

3.3. Effect analysis

In the on-off MT, the defects are hardly identified in raw images because of the uneven heating and noise, while the uneven heating and uneven emissivity effects can be decreased by some signal processing methods and the defect information is enhanced greatly in the resulting phase images.

From the visual point of view for Fig.4, the phase image acquired by IAC method is better than 4-point, DFS and correlation method.

To compare the methods quantitatively, the signal-to-noise ratio (SNR) defined as Eq.(40) was used.

$$S = |\overline{\varphi}_{\mathrm{d}} - \overline{\varphi}_{\mathrm{nd}}| / \sigma_{\mathrm{nd}} \qquad (40)$$

where $\overline{\varphi}_{\mathrm{d}}$ and $\overline{\varphi}_{\mathrm{nd}}$ are the mean pixel value (phase) in defect and non-defect area respectively, and σ_{nd} the standard deviation in non-defect area.

The selected defect areas, as indicated by two circles in Fig.3(i), are kept in the fixed positions while calculating the SNR of all the images listed in Fig.4. It can be seen from Fig.4 that:

(1) The phase solved by DFS is a real phase at a frequency, and its SNR is greater than 1, so DFS is a effective method.

(2) The SNR of the phase image solved by average 4-point method is less than 1, that means effect information is obscured by noise, thus, 4-point method is not fit for on-off MT well.

(3) Although the phase obtained by correlation coefficient method is not the real phase, the SNR, when reference signal comes from a cosine signal, approximates that of DFS. It means correlation coefficient method is effective.

(4) Although the phase obtained by IAC method is not the real phase, the defect information is clear for most reference-signal cases, and the SNR is greater. However, the detection effect depends on the reference signal to some extent.

4. Conclusion

(1) On-off MT is feasible to detect defects in composite materials.

(2) Four-point method and average four-point method are confined to process sinusodial (or cosine) signals and susceptible to noise. However, DFS (as equivalent as DFT and correlation method) method, correlation coefficient method and included angle cosine method can process any periodical signals and are not susceptible to noises, they are promising in on-off MT as well as in sinusoidal MT.

(3) The correlation coefficient method has the similar result with DFS if selecting a sinusoidal (or cosine) signal with the modulation frequency as the reference signal.

(4) The included angle cosine method is an effective method because the SNR is great and the way to choose the reference signal is more flexible than correlation coefficient method. The sinusoidal (or cosine) signal with the modulation frequency is firstly recommended as the reference signal.

ACKNOWLEDGMENTS

This work was supported by NSFC under project 50975016,60672101.

REFERENCES

[1] Robert L. Crane, Tommaso Astarita, et al. Aerospace Applications of Infrared and Thermal Testing, in book: Nondestructive Testing Handbook, Third Edition, Volum 3, Infrared and Thermal Testing, Edited by Patrick O. Moove, Xavier P. V. Maldague, American Society for Nondestructive Testing, 2001, 489-518

[2] Avdelidis N P, Almond D P, Dobbinson A, et al. Aircraft composites assessment by means of transient thermal NDT. Progress in Aerospace Sciences, 2004, 40: 143-162

[3] Ibarra-Castanedo C, Genest M, Guibert S, et al. Inspection of aerospace materials by pulsed thermography, lock-in thermography and vibrothermography: A comparative study[C]// Knettel K M, Vavilov V P, Miles J J. Proc SPIE Thermosense XXIX. Bellingham, WA: SPIE, 2007, 6541: 654116.1-9

[4] Maldague X, Marinetti S. Pulse Phase Infrared Thermography[J]. Journal of Applied Physics,1996,79(5): 2694~2698

[5] Meola C, Carlomagno G M, Squillace A, et al. Non-destructive evaluation of aerospace materials with lock-in thermography[J]. Engineering Failure Analysis, 2006, 13: 380-388

[6] Waldemar Swiderski. Lock-in Thermography to rapid evaluation of destruction area in composite materials used in military application[C]//Kenneth W. Tobin, Jr., Fabrice Meriaudeau. Proc SPIE–Sixth International Conference on Quality Control by Artificial Version. Bellingham, WA: SPIE, 2003, 5132: 506-517

[7] Burke M W, Miller W O, Status of vibroIR at Lawrence Livermore National Laboratory[C] // Burleigh D D, Cramer K E, Peacock G R. Proc SPIE-Thermosense XXVI. Bellingham,WA: SPIE, 2004, 5405: 313-321

[8] Takahide Sakagami, Shiro Kubo, Shiro Nakamura, et al. Application of lock-in data processing for thermographic NDT of concrete structures[C]// Maldague X P, Rozlosnik A E. Proc SPIE Thermosense XXIV. Bellingham, WA: SPIE, 2002, 4710: 552-557

[9] Guo Xingwang, Liu Yingtao, Guo Guangping, et al. Pulsed phase thermography and its application in the NDT of composite materials[J]. Journal of Beijing University of Aeronautics and Astronautics. 2005, 31(10): 1049-1053 (in Chinese)